

Article

# New Mononuclear Complex of Europium(III) and Benzoic Acid: From Synthesis and Crystal Structure Solution to Luminescence Emission

Carlos Hernández-Fuentes<sup>1</sup>, Rosario Ruiz-Guerrero<sup>1,\*</sup>, Angel de Jesús Morales-Ramírez<sup>1,2</sup> , Paulina Molina-Maldonado<sup>1</sup> and Dulce Y. Medina-Velazquez<sup>3</sup>

<sup>1</sup> Centro de Investigación e Innovación Tecnológica, Instituto Politécnico Nacional, cerrada de Cecati Sta. Catarina Azcapotzalco CP. 02250 CDMX, Mexico; carlosfhef@gmail.com (C.H.-F.); amoralesra@ipn.mx (A.d.J.M.-R.); mompau@gmail.com (P.M.-M.)

<sup>2</sup> Escuela Superior de Ingeniería Química e Industrias Extractivas, Instituto Politécnico Nacional, Av. Luis Enrique Erro S/N, Unidad Profesional Adolfo López Mateos, Zacatenco, GAM, C.P. 07738 CDMX, Mexico

<sup>3</sup> División de Ciencias Básicas e Ingeniería, Universidad Autónoma Metropolitana-Azcapotzalco, C.P. 02200 CDMX, Mexico; dyolotzin@correo.azc.uam.mx

\* Correspondence: maruizg@ipn.mx; Tel.: +52-55-5729-6000

Received: 7 July 2020; Accepted: 3 August 2020; Published: 4 August 2020



**Abstract:** This study presents a general method which can be used for the synthesis of mononuclear complexes with europium(III) and organic ligands with carboxylic groups. It describes the procedure for preparing a new mononuclear coordination complex with europium(III) and carboxylate ligands sourced from benzoic acid. The construction of mononuclear complexes with a coordination sphere saturated in carboxylic ligands must go through the preparation and purification of a europium(III) intermediate complex that presents a coordination sphere with anions that will be later exchanged for carboxylic groups and finally precipitated as a solvent-free or anion-free complex within the coordination sphere. The detailed synthesis procedure for powders of a new complex, as well as studies of its structural composition at each phase and luminescent properties, are detailed in this study. Analytical and spectroscopic data reveal the formation of a new mononuclear complex of the general formula  $[\text{Eu}(\text{OOC}\text{C}_6\text{H}_5)_3 \cdot (\text{HOOC}\text{C}_6\text{H}_5)_2]$ . The crystal structure of the Eu(III) complex was solved using X-ray powder diffraction data and EXPO2014 software, and the crystal structure result was deposited in the CCDC service with number 19771999.

**Keywords:** mononuclear compound; europium(III) carboxylate; benzoic acid

## 1. Introduction

In recent decades, there has been scientific and technological development regarding the use of lanthanides due to their versatility in different areas, including chemical analysis [1], catalysis [2] and biologic applications [3,4]. In particular, they are used for their luminescence properties, including highly pure color [5,6] and short radiative lifetimes [7]. Among the lanthanides, europium(III) stands out for its wide range of optical applications; however, the use of pure lanthanides is uncommon due to their low efficiency of direct absorption of the  $4f-4f$  states [8]. This problem can be solved with the use of ligands that provide an antenna effect, which is defined as a light conversion process via an absorption-energy transfer-emission sequence, where the ligand functions as a light collector and the metal ion emits energy [9–11].

Moreover, there is new interest in the use of organic ligands, especially carboxylic compounds [12–14]. These ligands are extensively studied because of the high kinetic and thermodynamic stability of their

corresponding lanthanide chelates [15], which have demonstrated to be efficient sensitizers when modified with light-harvesting moieties [16,17].

However, the most common use of carboxylic acids as ligands is as bidentate molecules, (dicarboxylic acids), which results in binuclear compounds, or even more lanthanide cations in its structure, [18–20] in which an indirect interaction between the metal centers through the ligands causes energy losses through non-radiative pathways [21]. It is also common to find in these complexes the presence of solvent in the coordination sphere of the final product, which does not favor luminescent emission mechanisms [22–25].

Of course, there are reports of mononuclear complexes [26,27], but it is not easy to get solvent-free compounds in the coordination sphere. In this study, we report a method for obtaining mononuclear complexes (free of solvents in their sphere of coordination) with organic ligands, specifically carboxylic ligands. The present work presents a newly developed method for the synthesis of mononuclear compounds that can easily absorb and conduct energy, avoiding the quenching effect caused by subtractor molecules of energy [28,29] and direct interactions between metallic centers [30].

For the method described in this paper, benzoic acid was used as organic ligand capable of coordinating with europium(III) to form a mononuclear species with this cation. This acid (Figure 1) presents in its structure an aromatic ring formed by conjugated bonds that facilitate the absorption of photons [31,32] as well as a carboxylic group (COOH) capable of chelating cations and facilitate the charge transfer to the metal ion. Overall, it is a molecule of relatively simple structure with the ability to absorb and transport UV radiation to the central ion.

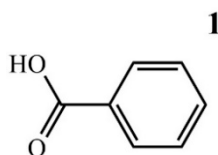


**Figure 1.** Chemical structure of benzoic acid: (1).

This study presents the synthesis, structural composition and luminescence properties of new europium(III) complex. The lanthanide is used as the central cation and benzoic acids are used exclusively as ligands. Detailed synthesis and characterization of the intermediate complex are presented due to the importance it represents in the construction of the final complex. The sum of the total procedure allows us to have a complete description of the methodology that can be followed for the construction of mononuclear complexes that are solvent-free in their coordination sphere and include lanthanide cations and carboxylic acids.

## 2. Experimental Section

Molecules of organic solvent in the coordination sphere pose an issue for practical luminescent devices because they act as load subtraction groups with low quantum efficiency [33]. Water was used as a solvent in the reaction because Europium chloride and benzoic acid have high solubility in this medium. In addition, water is an easy replacement molecule when it is in the coordination sphere [34]. The precipitation of the final complex was conducted in an ionic reaction medium favored by the presence of  $\text{Na}^+$  and  $\text{Cl}^-$  ions.

### 2.1. Materials and Methods

**Reagents:** The benzoic acid (99%), sodium hydroxide (99.9%) and europium(III) chloride (99%) used were supplied by Sigma-Aldrich (St. Louis, MI, USA). Deionized water was used as the only solvent.

**Methods:** The Fourier-transform infrared spectroscopy (FTIR) was performed on a Perkin Elmer Spectrum 65 FT-IR spectrometer using KBr pellets as support. The elemental analyses for C and H were carried out using a Thermo Scientific/Flash 2000 (Thermo Fisher Scientific Inc, Waltham, MA, USA)

elemental analyzer. A quantitative analysis was also conducted by atomic absorption spectrometry on a spectrometer AAnalyst 300 (Perkin Elmer, Waltham, MA, USA) to evaluate accurate percentages of europium(III) in synthesized europium(III) complexes. The mass spectrometry was performed on a MicrOTOF-Q II mass spectrometer (Bruker corporation, Billerica, MA, USA) using methanol as a solvent. The thermogravimetric analysis was obtained on STA 2500 equipment (NETZSCH-Gruppe, Selb, Germany) where about 10 mg of samples were heated at 5 °C/min from room temperature to 300 °C in a dynamic nitrogen atmosphere (flow rate = 50 mL/min). The melting point was determined by an IA 9000 (Electrothermal, Staffordshire, UK) series digital melting point apparatus. Scanning electron microscopy (SEM) was conducted on a JSM-7800 F Field Emission Scanning Electron microscope (Hitachi High-tech, Tokyo, Japan) operating at 10 keV. X-ray diffraction patterns were collected using a D8 Advance Eco powder diffractometer (Bruker corporation, Billerica, MA, USA) with Cu K $\alpha$  (1.54), with an angular range of 5° to 90° and a step size of 0.02. The determination of the unit cell parameters, identification of the space group, structure solution and model refinement via the Rietveld method, were carried out by EXPO2014 software (2014, Institute of Crystallography, Bari, Italy): a package able to automatically execute the full pathway of the powder solution process. The photoluminescence studies of the synthesized complex powders were recorded on an F-7000 FL spectrophotometer (Hitachi High-tech, Tokyo, Japan) equipped with a 150 W xenon lamp, at room temperature.

## 2.2. Synthesis

The first step gave rise to the complex **2** [Eu(OOCC<sub>6</sub>H<sub>5</sub>)<sub>3</sub>·(H<sub>2</sub>O)<sub>3</sub>], in which the bidentate interaction of three benzoate molecules with the metal ion results in the displacement of three chlorine molecules and three water molecules. In the second step, the water molecules still present in complex **2** were displaced by two benzoic acid molecules linked by monodentate coordinated bonds, to form complex **3** [Eu(OOCC<sub>6</sub>H<sub>5</sub>)<sub>3</sub>·(HOCC<sub>6</sub>H<sub>5</sub>)<sub>2</sub>], see Figure 2.

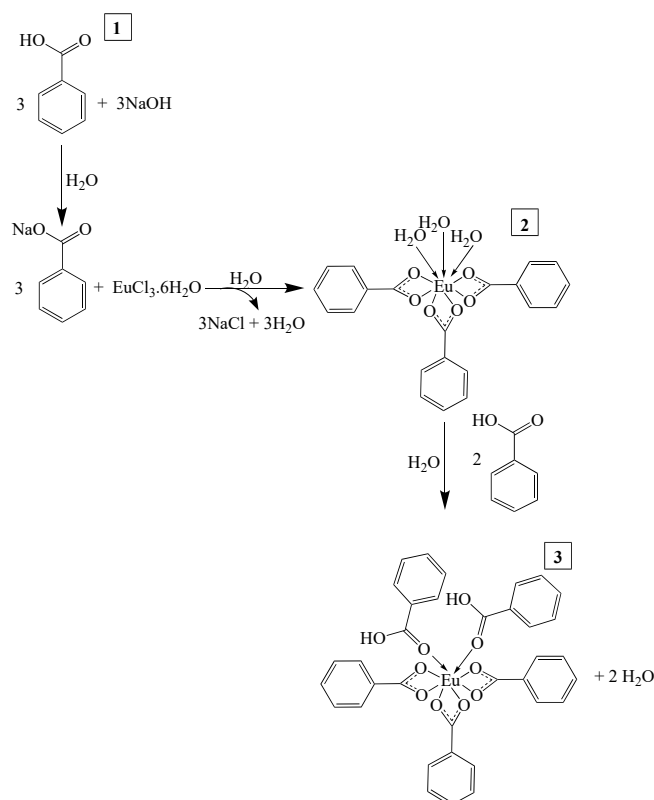


**Figure 2.** Synthesis of **2**: [Eu(OOCC<sub>6</sub>H<sub>5</sub>)<sub>3</sub>·(H<sub>2</sub>O)<sub>3</sub>] and **3**: [Eu(OOCC<sub>6</sub>H<sub>5</sub>)<sub>3</sub>·(HOCC<sub>6</sub>H<sub>5</sub>)<sub>2</sub>]. In both complexes, the oxidation state of europium is 3+.

### 2.2.1. Synthesis of Complex 2: $[\text{Eu}(\text{OOC}\text{C}_6\text{H}_5)_3 \cdot (\text{H}_2\text{O})_3]$

A sodium benzoate solution prepared from sodium hydroxide (3 mL, 1 mol L<sup>-1</sup>) and benzoic acid (1) solution (30 mL, 0.1 mol L<sup>-1</sup>) was reacted with europium(III) chloride (10 mL, 0.1 mol L<sup>-1</sup>) in an aqueous solution. The mixture was stirred for 6 h at room temperature to obtain complex 2. The precipitate was washed with deionized water and allowed to air dry (Figure 2).

$\text{Eu}(\text{OOC}\text{C}_6\text{H}_5)_3 \cdot (\text{H}_2\text{O})_3$  (2): Yield: 89%. Theoretical elemental analysis for C<sub>21</sub>H<sub>21</sub>O<sub>9</sub>Eu: C: 44.30%, H: 3.72%, Eu: 26.69%; Experimental: C: 44.61%, H: 3.68%, Eu: 27.12%.

### 2.2.2. Synthesis of Complex 3: $[\text{Eu}(\text{OOC}\text{C}_6\text{H}_5)_3 \cdot (\text{HOOC}\text{C}_6\text{H}_5)_2]$

First, 0.7 mmol of complex 2 dissolved in deionized water (30 mL) was added to an aqueous solution of benzoic acid (1.4 mmol in 30 mL) and stirred for 8 h. The precipitate obtained was washed with deionized water then allowed to dry at room temperature.

$\text{Eu}(\text{OOC}\text{C}_6\text{H}_5)_3 \cdot (\text{HOOC}\text{C}_6\text{H}_5)_2$  (3): Yield: 96%. Theoretical elemental analysis for C<sub>35</sub>H<sub>27</sub>O<sub>10</sub>Eu: C: 55.35%, H: 3.58%, Eu: 20.01%; Experimental: C: 55.64%, H: 3.52%, Eu: 19.60%.

## 3. Results and Discussion

The reaction was conducted to obtain the complexes 2 and 3 sequentially. Both complexes 2 and 3 were isolated and characterized by FTIR vibrational spectroscopy, thermogravimetric analysis, excitation, emission and luminescent decay curves. Complex 2 was characterized by mass spectrometry (ms/ms) and the X-ray diffraction pattern is shown for the complex 3.

### 3.1. Infrared Spectroscopy

Figure 3 shows the FTIR spectra of the benzoic acid used as precursor (1) and the complexes 2 and 3 are shown in Figure 2.

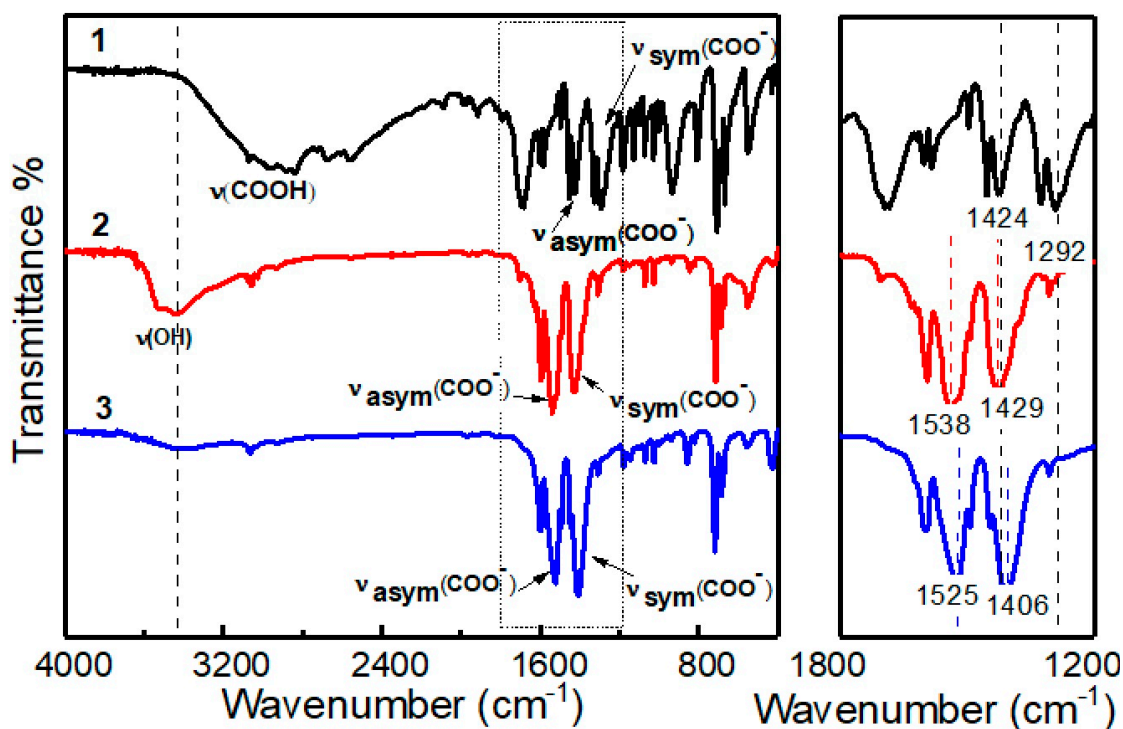


**Figure 3.** FTIR spectroscopy for 1: benzoic acid; 2:  $[\text{Eu}(\text{OOC}\text{C}_6\text{H}_5)_3 \cdot (\text{H}_2\text{O})_3]$ ; 3:  $[\text{Eu}(\text{OOC}\text{C}_6\text{H}_5)_3 \cdot (\text{HOOC}\text{C}_6\text{H}_5)_2]$ .

The nature of the obtained complexes was corroborated by infrared spectra. Figure 3 shows a shift of the carbonyl bond frequencies  $\nu$  ( $\text{COO}^-$ ) for the blank sample (1) and both complexes (2 and 3). The variations in the frequencies, both symmetric as asymmetric, of the  $\text{COO}^-$ -Eu bond-stretching band for complexes 2 ( $\nu_{\text{sym}} = 1429 \text{ cm}^{-1}$  and  $\nu_{\text{asym}} = 1538 \text{ cm}^{-1}$ ) and 3 ( $\nu_{\text{sym}} = 1406 \text{ cm}^{-1}$  and  $\nu_{\text{asym}} = 1525 \text{ cm}^{-1}$ ) were lower with respect to 1. The free coordination ligand is associated with the coordination of benzoyl to europium(III) [35].

The magnitude of the  $\Delta\nu$  value (Table 1) produced by each complex is related to the type of  $\text{COO}^-$  coordination character of the ligands associated with the Eu cation. Complex 2 presents the smallest value of this magnitude (109), which is lower than that presented by the benzoate 1 (132); this reflects the coordination to three benzoates as chelating ligands. An increase in this value to 119 for 3 indicates the additional coordination of two benzoic acid molecules in a monodentate form [36].

**Table 1.** Overview of synthesis identification.

Complex	Identification	Vibrations ( $\text{cm}^{-1}$ )			$\Delta\nu$ ( $\text{cm}^{-1}$ )
		$\nu$ (HO–H)	$\nu_{\text{asym}}$ ( $\text{COO}^-$ )	$\nu_{\text{sym}}$ ( $\text{COO}^-$ )	asym-sym
Benzoic acid <sup>a</sup>	1	–	1424	1292	132
[Eu(OOCC <sub>6</sub> H <sub>5</sub> ) <sub>3</sub> ·(H <sub>2</sub> O) <sub>3</sub> ]	2	3438	1538	1429	109
Eu(OOCC <sub>6</sub> H <sub>5</sub> ) <sub>3</sub> ·(HOCC <sub>6</sub> H <sub>5</sub> ) <sub>2</sub>	3	–	1525	1406	119

<sup>a</sup> precursor material evaluated as a blank.

According to previously indicated in the spectra of Figure 3, in complex 3, the band corresponding to the HO–H group of the coordinated water is no longer present, confirming its absence in the coordination sphere. By contrast, the spectrum on complex 2 shows a tension band corresponding to the HO–H of the three coordinated molecules at  $3420 \text{ cm}^{-1}$ . For its part, complex 2 presents a clear water signal in its sphere of coordination with a band at  $3400 \text{ cm}^{-1}$ .

In addition, mass spectroscopy studies of complex 2 show the characteristic losses of two molecules of water. The record of mass/mass technique of molecule 2 shows the fragmentation of the molecule and the molecular ion  $m/z = 551.03$ . The first loss of a water molecule is observed with the peak  $m/z = 533.02$  and the second loss of water at  $m/z = 515.01$ . It is worth mentioning that the same technique of characterization was not possible for complex 3 since the powder is insoluble in solvents that could be useful for this.

### 3.2. Thermogravimetric Analysis

In Figure 4a, the number of water molecules present in the powders of complex 2 was determined by the data obtained from the thermogravimetric analysis, which showed a 9.5% loss by weight at the temperature of  $100 \text{ }^\circ\text{C}$  as a result of the elimination of three water molecules (54.06 of 570.36), then continued stability until the temperature of  $300 \text{ }^\circ\text{C}$ . The inflexion point at  $241 \text{ }^\circ\text{C}$  corresponds to the phase change from a solid to a liquid of the compound, which is very close to the experimentally determined of  $242 \text{ }^\circ\text{C}$ .

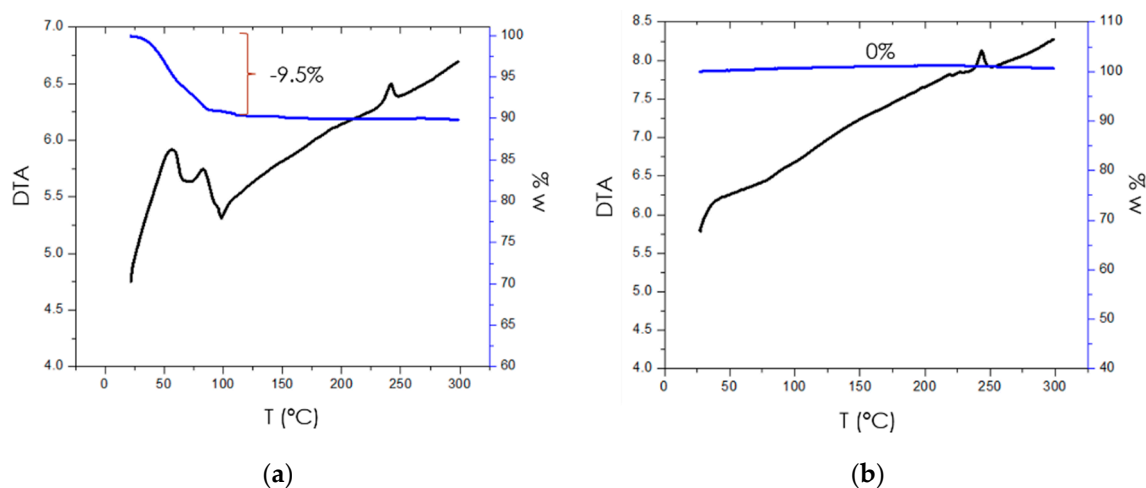
The powders of complex 3 were analyzed by thermogravimetry from  $24 \text{ }^\circ\text{C}$  to  $300 \text{ }^\circ\text{C}$  (Figure 4b) without weight loss, indicating the absence of water molecules. The data were corroborated with the FTIR results. The inflexion point at  $245 \text{ }^\circ\text{C}$  corresponds to the phase change from solid to liquid, which is very close to the experimentally determined of  $246 \text{ }^\circ\text{C}$ .

### 3.3. Morphologic Studies

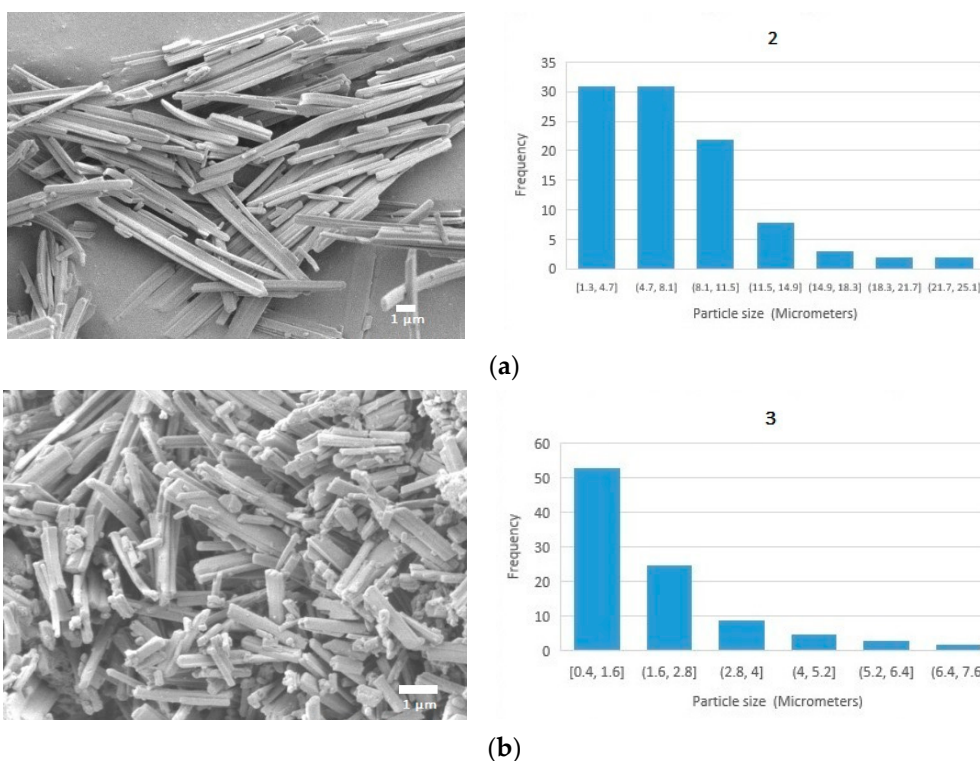
#### 3.3.1. Scanning Electron Microscopy

Figure 5a,b shows the particles of complex 2 and complex 3 by scanning electron microscopy (SEM), with a whiskers-like morphology and crystal shape characteristic typical of the triclinic space group [37]. For both cases, the SEM images and the non-symmetric unimodal graphics for the dispersion of sizes,

revealed that the whiskers tend to be smaller in the longitudinal direction, varying from 1.0  $\mu\text{m}$  to 2  $\mu\text{m}$  with a median longitudinal particle size ( $d_{50}$ ) of 6.7  $\mu\text{m}$  and longitudinal particle size distribution  $d_{80}$  of 11.1  $\mu\text{m}$  for the complex 2. For complex 3, the whisker sizes ranged from 4.0  $\mu\text{m}$  to 8.1  $\mu\text{m}$  with longitudinal particle size distributions  $d_{50}$  of 1.6  $\mu\text{m}$  and  $d_{80}$  of 2.9  $\mu\text{m}$ . The radial particle size presented an average size of 0.5  $\mu\text{m}$  for complex 2 and 0.6  $\mu\text{m}$  for complex 3.



**Figure 4.** Thermogravimetric analysis. (a) 2:  $[\text{Eu}(\text{OOC}\text{C}_6\text{H}_5)_3 \cdot (\text{H}_2\text{O})_3]$ ; (b) 3:  $[\text{Eu}(\text{OOC}\text{C}_6\text{H}_5)_3 \cdot (\text{HOOC}\text{C}_6\text{H}_5)_2]$ .



**Figure 5.** Scanning electron microscopy. (a) 2:  $[\text{Eu}(\text{OOC}\text{C}_6\text{H}_5)_3 \cdot (\text{H}_2\text{O})_3]$ ; (b) 3:  $[\text{Eu}(\text{OOC}\text{C}_6\text{H}_5)_3 \cdot (\text{HOOC}\text{C}_6\text{H}_5)_2]$ .

### 3.3.2. X-ray Powder Diffraction Data

Various crystallization systems were used to obtain solvent-free monocrystals in the coordination sphere without any success. Therefore, the X-ray powder diffraction was used.

### 3.4. Crystal Structure Solution

EXPO2014 [38] was used in the solution and refined process of the structure. EXPO2014 integrates a package to index a powder diffraction pattern, extraction of integrated intensities, determination of the space group, the solution of crystal structure through direct methods and/or direct space approach and refinement of the structure using the Rietveld method.

The indexing of the X-ray diffraction pattern of **3** was obtained through the N-TREOR09 computer program integrated through EXPO2014. The approximate unit cell parameters were calculated from the 31 major peaks. The space group determination step gave triclinic *P*-1 space group with two molecules in the unit cell. The solution was carried out by the direct space method, which involved the generation of a random sequence of test structures from an appropriate 3D model (drawn by ChemBioDraw Ultra 13.0 and optimized in MOPAC [39] by the RM1 model, which was moved until a good match was found between the calculated and observed pattern ( $X^2 = 1.564$ ) (Figure 6).

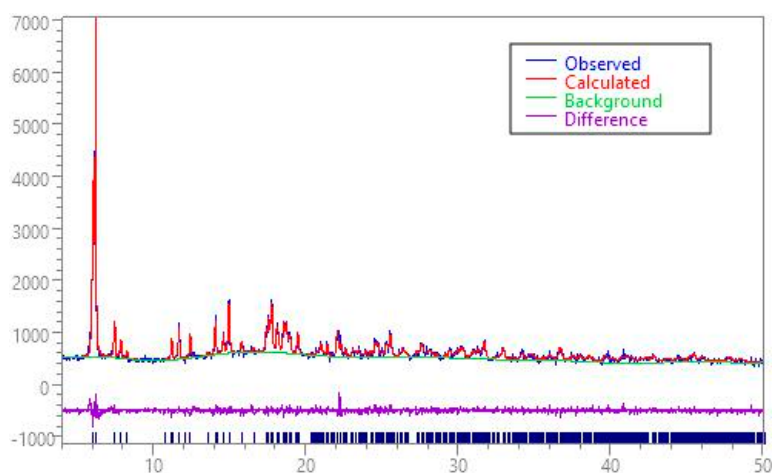


**Figure 6.** Rietveld plot of **3** [Eu(OOCC<sub>6</sub>H<sub>5</sub>)<sub>3</sub>·(HOCC<sub>6</sub>H<sub>5</sub>)<sub>2</sub>]. (blue line) Observed diffraction profile; (red line) calculated profile; (green line) background and (violet line) difference profile.

The model was refined by the Rietveld method and the optimized crystal structure is shown in Figure 7.

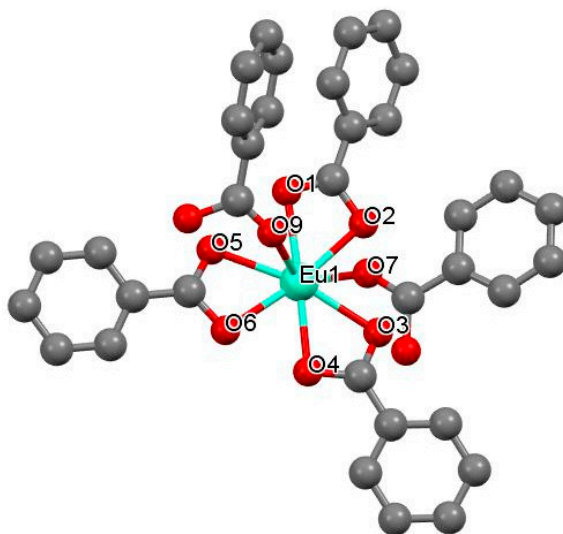


**Figure 7.** Crystal structure of complex **3**: [Eu(OOCC<sub>6</sub>H<sub>5</sub>)<sub>3</sub>·(HOCC<sub>6</sub>H<sub>5</sub>)<sub>2</sub>]. Hydrogen atoms are omitted for clarity.

In the crystal structure, each atom of Europium, independent of each other, is bidentally linked to three benzoate anions and connected through monodentate to two carboxylic acid molecules. The packing seems to be influenced by  $\pi\cdots\pi$  interactions (Figure 8). Neighboring benzoic acid rings are at 3.471 Å distances (centroid-to-centroid) with slippage of 0.41 Å.

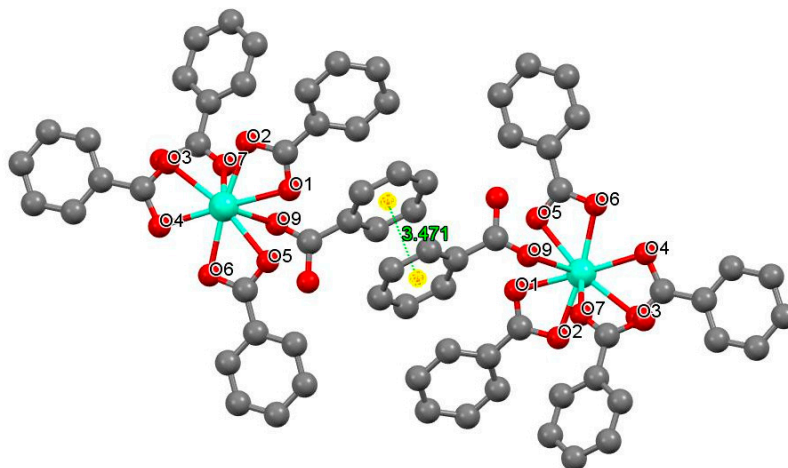


**Figure 8.** Crystal packing of complex 2, showing  $\pi\cdots\pi$  interactions.

Table 2 shown the Eu–O distances, the range from 2.3001 Å (Eu–O2) to 2.3895 Å (Eu–O3) are in good agreement with similar Eu–O bond distances as found in powder X-ray structures from the Cambridge Crystallographic Data Center [40,41].

**Table 2.** Bond distances europium–oxygen (Å) for complex 3.

Bond Distances of Europium–Oxygen(Å)			
Eu–O1 2.3637(3)	Eu–O3 2.3895(2)	Eu–O5 2.3866(3)	Eu–O7 2.3409(2)
Eu–O2 2.3001(2)	Eu–O4 2.3324(3)	Eu–O6 2.3236(2)	Eu–O9 2.3347(2)

The resolution parameters for complex 3 are shown in Table 3 and CCDC 19771999 contains the supplementary crystallographic data for this study. These data can be obtained free of charge from the Cambridge Crystallographic Data Center (CCDC) via [www.ccdc.cam.ac.uk/structures](http://www.ccdc.cam.ac.uk/structures).

**Table 3.** Crystal data, Rietveld refinement parameters and Cambridge Crystallographic Data Center (CCDC) depository number for complex 3:  $[\text{Eu}(\text{OCC}_6\text{H}_5)_3 \cdot (\text{HOCC}_6\text{H}_5)_2]$ .

Formula, molecular weight	Eu C <sub>35</sub> H <sub>27</sub> O <sub>10</sub> , 760.56
Temperature (K), (Å)	293, 1.54056
System, space group	Triclinic, <i>P</i> -1
a, b, c (Å); $\alpha$ , $\beta$ , $\gamma$ (°)	24.496(3), 15.166(2), 5.0934(8), 92.408(1), 91.007(3), 74.814(6),
V (Å <sup>3</sup> ), Z	1824.42, 2
2 $\theta$ range, step (°)	4–40, 0.02
Nr. of data points	3701
Nr. of Bragg refl., parameters	884, 112
Rp (%), Rwp (%), X <sup>2</sup>	3.876, 5.032, 1.564
Rexp (%), R <sub>Bragg</sub> (%)	4.024, 1.397
CCDC depository nr.	CCDC 19771999

### 3.5. Luminescence Studies: Excitation and Emission Spectra

#### 3.5.1. Excitation and Emission Spectra

The excitation spectra of the complexes are shown in Figure 9, which were performed with  $\lambda_{em} = 616$  nm. It includes a broad band assigned to the  $S_0 \rightarrow S_1$  ( $\pi, \pi^*$ ) transition centered at 290 nm in complex 2 and 288 nm in complex 3, and on the right side, excitations correspond to the absorption bands that originated from the  ${}^7F_0$  ground state to the excited level  ${}^5L_7$  centered at 393 nm. In complex 3, this last excited level is, in terms of intensity, higher than in complex 2 (i.e., the area under the curve shows 70% more energy absorption in complex 3 than in complex 2), indicating the potential contribution of an energy ligand to the metal charge transfer states (LMCTS) of the two additional ligands. This corresponds to the antenna effect; at this wavelength, it absorbs the ligand and subsequently transfers the energy to the  $Eu^{3+}$  ion.

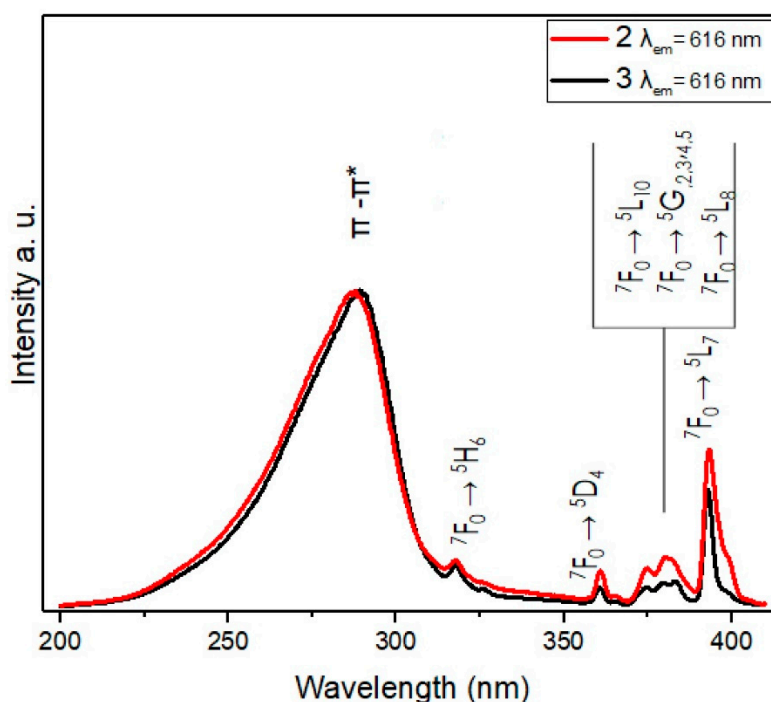


**Figure 9.** Excitation spectrum with  $\lambda_{em} = 616$  nm, for 2:  $[Eu(OOCC_6H_5)_3 \cdot (H_2O)_3]$  and 3:  $[Eu(OOCC_6H_5)_3 \cdot (HOCC_6H_5)_2]$ .

Figure 10 shows the emission spectra of both compounds of europium(III). The compound containing five carboxylic groups presents higher emission, even when it has the same europium(III) ( $5 \times 10^{-3}$  mmol). This effect can be explained by the fact that by presenting a greater number of ligands, complex 3 allows a greater transfer of energy towards the luminescent center, as observed in the excitation spectrum. Conversely, the intensity of the  ${}^5D_0 \rightarrow {}^7F_1$  magnetic dipole transition (centered at 592 nm) is independent of the surroundings of the  $Eu^{3+}$ , whereas the intensity of the  ${}^5D_0 \rightarrow {}^7F_2$  electric dipole transition (centered at 616 nm) is very sensitive to site symmetry [42]. In both complexes, the area under the curve was calculated using integration for the  ${}^5D_0 \rightarrow {}^7F_2$  transition. It was determined that complex 3 presents 15% more energy emission than complex 2.

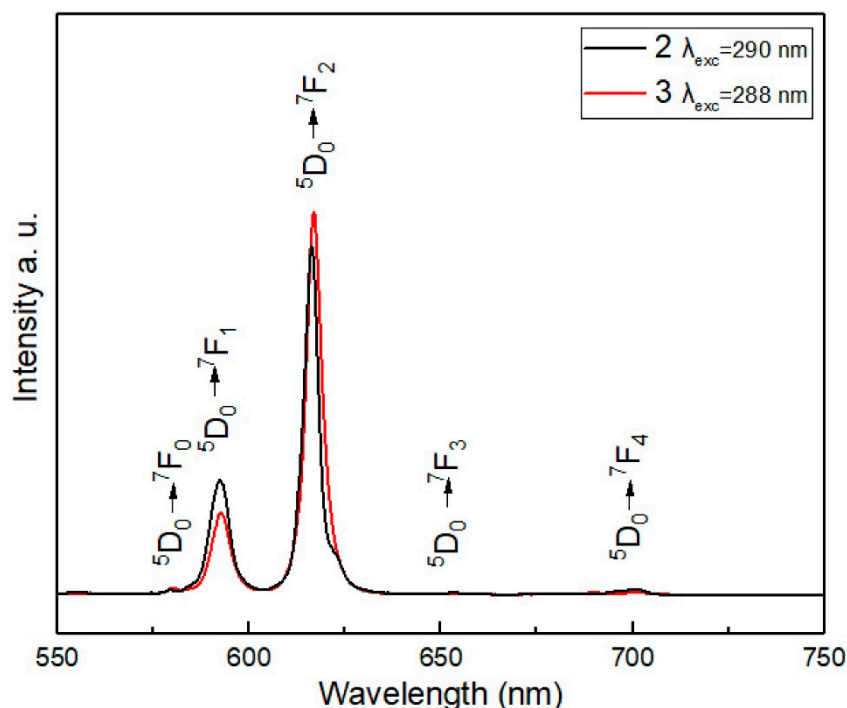


**Figure 10.** Emission spectrum, with  $\lambda_{\text{exc}} = 290$  nm, for **2**:  $[\text{Eu}(\text{OOC}\text{C}_6\text{H}_5)_3 \cdot (\text{H}_2\text{O})_3]$  and **3**:  $[\text{Eu}(\text{OOC}\text{C}_6\text{H}_5)_3 \cdot (\text{HOOC}\text{C}_6\text{H}_5)_2]$ .

Moreover, it is possible to set the ratio  $R = I(5D_0 \rightarrow 7F_2)/I(5D_0 \rightarrow 7F_1)$  as a reference to the coordination state and symmetry. Since the intensity  $5D_0 \rightarrow 7F_2$  increases with the decreasing of the site symmetry. If the  $R$  value is low, the  $\text{Eu}^{3+}$  cation tends to localize in a centrosymmetric site or at a high symmetry site. In contrast, when the  $R$  value is high, the  $\text{Eu}^{3+}$  cation tends to localize in non-centrosymmetric site or at a low symmetry site [43,44]. The  $R$  factor increases from 2.41 in complex **2** to 3.89 in complex **3**, which shows that the  $\text{Eu}^{3+}$  cation is in a position of less symmetry in complex **3**. Then, the energy in complex **3** prefers the  $5D_0 \rightarrow 7F_2$  transition to the  $5D_0 \rightarrow 7F_1$  transition because of the influence of the local symmetry, effect of the two extra ligands.

Moreover, the observed broadening of the  $5D_0 \rightarrow 7F_2$  band on complex **3** indicates that  $\text{Eu}^{3+}$  cations are located inhomogeneously at those sites without inversion symmetry [45,46]. Another important factor is the absence of water molecules, which acts as energy subtractors since the emission level decreases strongly through coupling with the excited vibratory levels of the OH oscillator of the coordinated water molecules [33].

Figure 11 shows the Jablonski partial energy diagram of complex **3** excited at 290 nm. The emission peaks, observed in Figure 10, appearing as the five typical bands at approximately 580 nm, 592 nm, 616 nm, 653 nm and 700 nm correspond to the characteristic emission transitions  $5D_0 \rightarrow 7FJ$  ( $J = 0, 1, 2, 3, 4$ ) [47]. The intramolecular energy transfer from the  $S_0 \rightarrow S_1$  ( $\pi, \pi^*$ ) state of the ligand to the excited state of  $\text{Eu}(\text{III})$  is promoted by the excitation energy of the ligand during the photoluminescence.

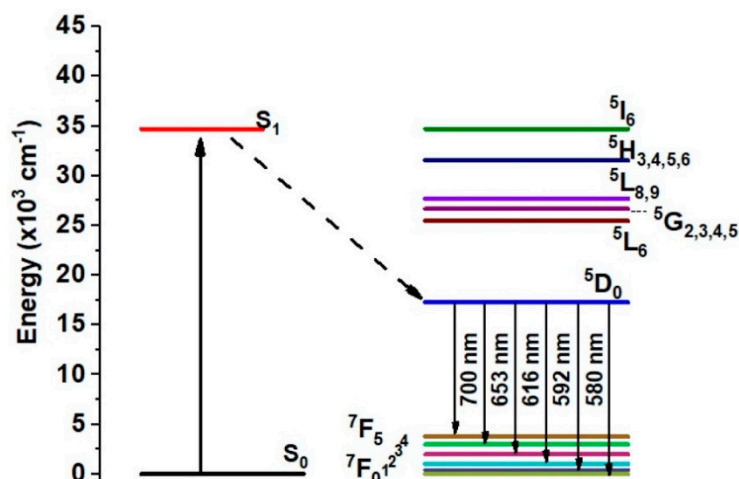


Figure 11. Partial energy level diagram of 3:  $[\text{Eu}(\text{OCC}_6\text{H}_5)_3 \cdot (\text{HOCC}_6\text{H}_5)_2]$ .

### 3.5.2. Luminescence Decay Profiles

The decay lifetime curves of the Eu(III) for both complexes are shown in Figure 12, with emission monitored at 616 nm with a 290 nm excitation energy. The observed mono-exponential fitting (goodness of fit,  $R^2 = 0.99991$  and  $0.9996$  for 2 and 3, respectively) indicates that both complexes present a homogeneous composition [48]. The average life ( $\tau_{av}$ ) increases from 0.42 ms in 2 to 0.53 ms in 3. The change of the symmetry from higher to lower modifies the luminescence spectrum and shortens the radiative lifetime [49]. This effect can be explained since the two extra carboxylic acids in the coordination sphere provide the function of a chelating agent, prevent nonradiative transitions and produce better use of energy in the form of light, thereby increasing decay time. In addition, it is well known that water molecules serve as quenching sites in many Eu(III) carboxylate complexes when they are at the coordination sphere due to can efficiently non-radiatively depopulate the  $^5\text{D}_0$  excited state of  $\text{Eu}^{3+}$  [50,51].

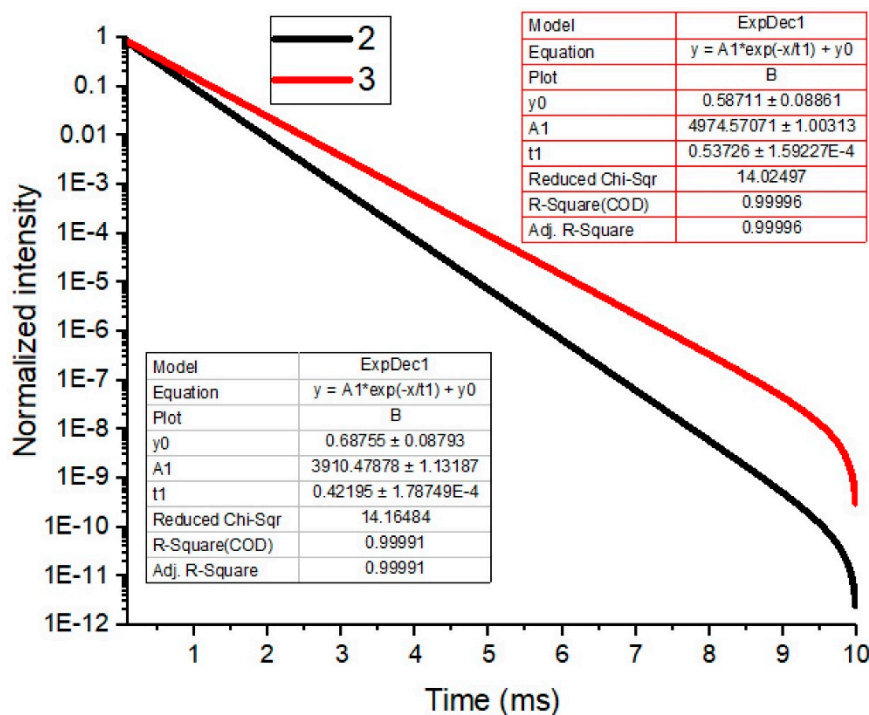


Figure 12.  $^5\text{D}_0 \rightarrow ^7\text{F}_2$  level decay time profile at 393 nm of complex 2:  $[\text{Eu}(\text{OCC}_6\text{H}_5)_3 \cdot (\text{H}_2\text{O})_3]$  and complex 3:  $[\text{Eu}(\text{OCC}_6\text{H}_5)_3 \cdot (\text{HOCC}_6\text{H}_5)_2]$ .

#### 4. Conclusions

In this study, a new mononuclear compound of europium(III) with benzoic acid as the ligand and a full, solvent-free coordination sphere as the main feature was synthesized: [Eu(OOCC<sub>6</sub>H<sub>5</sub>)<sub>3</sub>·(HOCC<sub>6</sub>H<sub>5</sub>)<sub>2</sub>].

The synthesis of this complex was conducted in two stages in which the formation of an intermediate compound [Eu(OOCC<sub>6</sub>H<sub>5</sub>)<sub>3</sub>·(H<sub>2</sub>O)<sub>3</sub>] is necessary to achieve the purity of the compound and a solvent-free structure. Both compounds were fully characterized and their photophysical properties compared. The main compound and the intermediate complex were widely characterized to corroborate the formation of the structure and mainly to see how the full sphere of coordination and the absence of water as a solvent with charge subtractor characteristics influenced the luminescent properties of the compound. Both compounds showed luminescent absorption in the region of 290 nm (290 in complex 2 and 288 in complex 3) assigned to the S<sub>0</sub>–S<sub>1</sub> (π, π\*) transition and an emission centered on 616 nm (corresponding to transition <sup>5</sup>D<sub>0</sub> → <sup>7</sup>F<sub>2</sub>) with red light emission characteristics. The <sup>5</sup>D<sub>0</sub> → <sup>7</sup>F<sub>2</sub> the hypersensitive transition band and its intensity are much more influenced by the local symmetry of the Eu<sup>3+</sup> ion due to the interactions of the ligand with the ion. This interaction is greater in complex 3 than in complex 2 due to the apparent chelating action of the two additional ligands that promote better use of energy and prevent energy losses by non-radiative routes. The complete coordination compound showed a 15% increase in the emission, showing greater luminescent capacities. Decay times suggest a better use of absorbed light, as the time in the main compound is longer. In some way, the chelating action ensures a greater transfer of the ligands to the central ion, avoiding the loss of energy by non-radiative transitions. A structure with a coordination sphere full of carboxylic acids and free of water has better use of energy in the form of light. The two-stage method described in this study has the potential to be used for the synthesis of mononuclear europium(III) complexes with different carboxylic acids as ligands.

**Author Contributions:** Conceptualization, R.R.-G.; Formal Analysis, A.d.J.M.-R. and D.Y.M.-V.; Investigation, P.M.-M.; Methodology, C.H.-F. All authors have read and agreed to the published version of the manuscript.

**Funding:** This research was funded by the National Polytechnic Institute, SIP projects 20201463 and 20201512.

**Conflicts of Interest:** The authors declare no conflict of interest.

#### References

1. Doat, A.; Fanjul, M.; Pellé, F.; Hollande, E.; Lebugle, A. Europium-doped bioapatite: A new photostable biological probe, internalizable by human cells. *Biomaterials* **2003**, *24*, 3365–3371. [[CrossRef](#)]
2. Lai, J.; Wang, T.; Zhang, H.; Ye, L.; Yan, C.; Gu, W. Modulating the photoluminescence of europium oxide nanoparticles by controlling thermal decomposition conditions. *J. Lumin.* **2019**, *214*, 116534. [[CrossRef](#)]
3. Zou, Y.; Sun, F.; Liu, C.; Yu, C.; Zhang, M.; He, Q.; Xiong, Y.; Xu, Z.; Yang, S.; Liao, G. A novel nanotheranostic agent for dual-mode imaging-guided cancer therapy based on europium complexes-grafted-oxidative dopamine. *Chem. Eng. J.* **2019**, *357*, 237–247. [[CrossRef](#)]
4. Xuan, Y.; Song, X.L.; Yang, X.Q.; Zhang, R.Y.; Song, Z.Y.; Zhao, D.H.; Hou, X.L.; An, J.; Zhang, X.S.; Zhao, Y. Di Bismuth particles imbedded degradable nanohydrogel prepared by one-step method for tumor dual-mode imaging and chemo-photothermal combined therapy. *Chem. Eng. J.* **2019**, *375*, 122000. [[CrossRef](#)]
5. Decadt, R.; Van Hecke, K.; Depla, D.; Leus, K.; Weinberger, D.; Van Driessche, I.; Van Der Voort, P.; Van Deun, R. Synthesis, Crystal Structures, and Luminescence Properties of Carboxylate Based Rare-Earth Coordination Polymers. *Inorg. Chem.* **2012**, *51*, 11623–11634. [[CrossRef](#)]
6. Singh, R.; King, A.; Nayak, B.B. Reddish emission of europium doped zinc oxide nanophosphor prepared through precipitation route using sodium borohydride. *J. Alloys Compd.* **2019**, *792*, 1191–1199. [[CrossRef](#)]
7. Xu, H.; Sun, Q.; An, Z.; Wei, Y.; Liu, X. Electroluminescence from europium(III) complexes. *Coord. Chem. Rev.* **2015**, *293–294*, 228–249. [[CrossRef](#)]
8. Binnemans, K. Interpretation of europium(III) spectra. *Coord. Chem. Rev.* **2015**, *295*, 1–45. [[CrossRef](#)]

9. Mech, A.; Karbowski, M.; Görrler-Walrand, C.; Van Deun, R. The luminescence properties of three tetrakis dibenzoylmethane europium(III) complexes with different counter ions. *J. Alloys Compd.* **2008**, *451*, 215–219. [[CrossRef](#)]
10. Pham, Y.H.; Trush, V.A.; Amirkhanov, V.M.; Gawryszewska, P. Structural and spectroscopic study of the europium complex with N-(diphenylphosphoryl)pyrazine-2-carboxamide. *Opt. Mater.* **2017**, *74*, 197–200. [[CrossRef](#)]
11. Akerboom, S.; Meijer, M.S.; Siegler, M.A.; Fu, W.T.; Bouwman, E. Structure, Photo-and triboluminescence of the lanthanoid dibenzoylmethanates: HNEt<sub>3</sub>[Ln(dbm)<sub>4</sub>]. *J. Lumin.* **2014**, *145*, 278–282. [[CrossRef](#)]
12. Hilder, M.; Lezhnina, M.; Junk, P.C.; Kynast, U.H. Spectroscopic properties of lanthanoid benzene carboxylates in the solid state: Part 3. N-heteroaromatic benzoates and 2-furanates. *Polyhedron* **2013**, *52*, 804–809. [[CrossRef](#)]
13. Lee, B.H.; Chung, K.H.; Shin, H.S.; Park, Y.J.; Moon, H. Europium(III) complexes of polyfunctional carboxylic acids: Luminescence probes of possible binding sites in fulvic acid. *J. Colloid Interface Sci.* **1997**, *188*, 439–443. [[CrossRef](#)]
14. Bergbreiter, D.E.; Poteat, J.L.; Zhang, L. Complexation of europium using polyethylene carboxylic acid. *React. Polym.* **1993**, *20*, 99–109. [[CrossRef](#)]
15. Feng, J.; Zhang, H. Hybrid materials based on lanthanide organic complexes: A review. *Chem. Soc. Rev.* **2013**, *42*, 387–410. [[CrossRef](#)] [[PubMed](#)]
16. Reddy, M.L.P.; Sivakumar, S. Lanthanide benzoates: A versatile building block for the construction of efficient light emitting materials. *Dalt. Trans.* **2013**, *42*, 2663–2678. [[CrossRef](#)]
17. Nakajima, A.; Nakanishi, T.; Kitagawa, Y.; Seki, T.; Ito, H.; Fushimi, K.; Hasegawa, Y. Hyper-stable organo-Eu III luminophore under high temperature for photo-industrial application. *Sci. Rep.* **2016**, *6*, 1–9. [[CrossRef](#)]
18. Ramya, A.R.; Reddy, M.L.P.; Cowley, A.H.; Vasudevan, K.V. Synthesis, crystal structure, and photoluminescence of homodinuclear lanthanide 4-(dibenzylamino)benzoate complexes. *Inorg. Chem.* **2010**, *49*, 2407–2415. [[CrossRef](#)]
19. Carter, K.P.; Thomas, K.E.; Pope, S.J.A.; Holmberg, R.J.; Butcher, R.; Murugesu, M.; Cahill, C.L. Supramolecular Assembly of Molecular Rare-Earth-3,5-Dichlorobenzoic Acid-2,2':6',2''-Terpyridine Materials: Structural Systematics, Luminescence Properties, and Magnetic Behavior. *Inorg. Chem.* **2016**, *55*, 6902–6915. [[CrossRef](#)]
20. Carter, K.P.; Pope, S.J.A.; Cahill, C.L. A series of Ln-p-chlorobenzoic acid-terpyridine complexes: Lanthanide contraction effects, supramolecular interactions and luminescent behavior. *CrystEngComm* **2014**, *16*, 1873–1884. [[CrossRef](#)]
21. Allendorf, M.D.; Bauer, C.A.; Bhakta, R.K.; Houk, R.J.T. Luminescent metal-organic frameworks. *Chem. Soc. Rev.* **2009**, *38*, 1330–1352. [[CrossRef](#)] [[PubMed](#)]
22. Xiao, P.; Zhang, J.J.; Wang, Z.Q.; Lin, H. Photon Conversion and Radiation Synergism in Eu/Tb Complexes Incorporated Poly Methyl Methacrylate. *Adv. Mater. Sci. Eng.* **2016**, *2016*, 2618253. [[CrossRef](#)]
23. Wang, Z.M.; Van De Burgt, L.J.; Choppin, G.R. Spectroscopic study of lanthanide(III) complexes with carboxylic acids. *Inorg. Chim. Acta* **1999**, *293*, 167–177. [[CrossRef](#)]
24. Champness, N.R. The future of metal-organic frameworks. *Dalt. Trans.* **2011**, *40*, 10311–10315. [[CrossRef](#)] [[PubMed](#)]
25. Utochnikova, V.V.; Solodukhin, N.N.; Aslandukov, A.N.; Marciniak, L.; Bushmarinov, I.S.; Vashchenko, A.A.; Kuzmina, N.P. Lanthanide tetrafluorobenzoates as emitters for OLEDs: New approach for host selection. *Org. Electron. Phys. Mater. Appl.* **2017**, *44*, 85–93. [[CrossRef](#)]
26. Fiedler, T.; Hilder, M.; Junk, P.C.; Kynast, U.H.; Lezhnina, M.M.; Warzala, M. Synthesis, structural and spectroscopic studies on the lanthanoid p-aminobenzoates and derived optically functional polyurethane composites. *Eur. J. Inorg. Chem.* **2007**, *2007*, 291–301. [[CrossRef](#)]
27. Chen, X.-F.; Duan, C.-Y.; Zhu, X.-H.; You, X.-Z.; Raj, S.S.S.; Fun, H.-K.; Wu, J. Triboluminescence and crystal structures of europium(III) complexes. *Mater. Chem. Phys.* **2001**, *72*, 11–15. [[CrossRef](#)]
28. Zhang, J.; Wang, L.X.; Zhang, L.; Chen, Y.; Zhang, Q.T. Co-luminescence properties of terbium ions-benzoic acid-phen complexes doped with europium ions. *Rare Met.* **2013**, *32*, 599–604. [[CrossRef](#)]
29. Borges, A.S.; Dutra, J.D.L.; Freire, R.O.; Moura, R.T.; Da Silva, J.G.; Malta, O.L.; Araujo, M.H.; Brito, H.F. Synthesis and characterization of the europium(III) pentakis(picrate) complexes with imidazolium counterions: Structural and photoluminescence study. *Inorg. Chem.* **2012**, *51*, 12867–12878. [[CrossRef](#)]
30. Baldo, M.A.; O'Brien, D.F.; You, Y.; Shoustikov, A.; Sibley, S.; Thompson, M.E.; Forrest, S.R. Highly efficient phosphorescent emission from organic electroluminescent devices. *Nature* **1998**, *395*, 151–154. [[CrossRef](#)]

31. Hilder, M.; Junk, P.C.; Kynast, U.H.; Lezhnina, M.M. Spectroscopic properties of lanthanoid benzene carboxylates in the solid state: Part 1. *J. Photochem. Photobiol. A Chem.* **2009**, *202*, 10–20. [[CrossRef](#)]
32. de Oliveira, T.C.; Santos, H.P.; Lahoud, M.G.; Franco, D.F.; Freire, R.O.; Dutra, J.D.L.; Cuin, A.; de Lima, J.F.; Marques, L.F. Elucidating the energy transfer process in mononuclear and binuclear lanthanide complexes of the anti-inflammatory drug ibuprofen: From synthesis to high luminescence emission. *J. Lumin.* **2017**, *181*, 196–210. [[CrossRef](#)]
33. Albuquerque, R.Q.; Freire, R.O.; Malta, O.L. On the use of ligand field parameters in the study of coordinated water molecules in Eu<sup>3+</sup> complexes. *J. Phys. Chem. A* **2005**, *109*, 4607–4610. [[CrossRef](#)] [[PubMed](#)]
34. Abdel-Mottaleb, M.S.A.; Galal, H.R.; Dessouky, A.F.M.; El-Naggar, M.; Mekkawi, D.; Ali, S.S.; Attya, G.M. Fluorescence and photostability studies of anthracene-9-carboxylic acid in different media. *Int. J. Photoenergy* **2000**, *2*, 47–53. [[CrossRef](#)]
35. Yu, Z.; Guo, J.; Li, D.; Lin, H. Multiligand Europium Complexes Incorporated Polyvinylpyrrolidone for Enhanced Solar Cell. *Adv. Mater. Sci. Eng.* **2019**, *2019*, 6180656. [[CrossRef](#)]
36. Deacon, G.B.; Phillips, R.J. Relationships between the carbon-oxygen stretching frequencies of carboxylate complexes and the type of carboxylate coordination. *Coord. Chem. Rev.* **1980**, *33*, 227–250. [[CrossRef](#)]
37. Strelcov, E.; Kolmakov, A. Chemical sensors from lead metallophthalocyanine whiskers. *Proc. IEEE Sensors* **2007**, *2*, 636–639. [[CrossRef](#)]
38. Altomare, A.; Cuocci, C.; Giacovazzo, C.; Moliterni, A.; Rizzi, R.; Corriero, N.; Falcicchio, A. EXPO2013: A kit of tools for phasing crystal structures from powder data. *J. Appl. Crystallogr.* **2013**, *46*, 1231–1235. [[CrossRef](#)]
39. Stewart Computational Chemistry—MOPAC Home Page. Available online: <http://www.openmopac.net/index.html> (accessed on 20 May 2020).
40. Jiang, W.; Hong, C.; Wei, H.; Wu, Z.; Ye, S.; Huang, C.-H. A green-emitting iridium complex used for sensitizing europium ion with high quantum yield. *Inorg. Chim. Acta* **2017**, *459*, 124–130. [[CrossRef](#)]
41. Wang, A.-L.; Zhou, D.; Chen, Y.-N.; Li, J.J.; Zhang, H.-X.; Zhao, Y.-L.; Chu, H. Crystal structure and photoluminescence of europium, terbium and samarium compounds with halogen-benzoate and 2,4,6-tri(2-pyridyl)-s-triazine. *J. Lumin.* **2016**, *177*, 22–30. [[CrossRef](#)]
42. Hreniak, D.; Speghini, A.; Bettinelli, M.; Streck, W. Spectroscopic investigations of nanostructured LiNbO<sub>3</sub> doped with Eu<sup>3+</sup>. *J. Lumin.* **2006**, *119–120*, 219–223. [[CrossRef](#)]
43. Medina, D.Y.; Orozco, S.; Hernandez, I.; Hernandez, R.T.; Falcony, C. Characterization of europium doped lanthanum oxide films prepared by spray pyrolysis. *J. Non-Cryst. Solids* **2011**, *357*, 3740–3743. [[CrossRef](#)]
44. García, R.N.; Desirena, H.; López-Luke, T.; Guerrero-Contreras, J.; Jayasankar, C.; Quintero-Torres, R.; De La Rosa, E. Spectroscopic properties of Eu<sup>3+</sup>/Nd<sup>3+</sup> co-doped phosphate glasses and opaque glass-ceramics. *Opt. Mater.* **2015**, *46*, 34–39. [[CrossRef](#)]
45. Crystal, P.H.; Fujihara, S.; Tokumo, K. Multiband Orange-Red Luminescence of Eu<sup>3+</sup> Ions Based on the Pyrochlore-Structured Host Crystal. *Chem. Mater.* **2005**, *17*, 5587–5593.
46. Yang, C.; Fu, L.-M.; Wang, Y.; Zhang, J.-P.; Wong, W.-T.; Ai, X.-C.; Qiao, Y.-F.; Zou, B.-S.; Gui, L.-L. A Highly Luminescent Europium Complex Showing Visible-Light-Sensitized Red Emission: Direct Observation of the Singlet Pathway. *Angew. Chem.* **2004**, *116*, 5120–5123. [[CrossRef](#)]
47. Yan, B.; Song, Y.S. Spectroscopic study on the photophysical properties of lanthanide complexes with 2,2'-bipyridine-N, N'-dioxide. *J. Fluoresc.* **2004**, *14*, 289–294. [[CrossRef](#)]
48. Wu, M.; You, J.; Song, Z. Luminescence Study of the Interaction of Carboxymethyl Chitosan with Metal Ions. *J. Appl. Spectrosc.* **2014**, *81*, 602–606. [[CrossRef](#)]
49. Shavaleev, N.M.; Eliseeva, S.V.; Scopelliti, R.; Bünzli, J.-C.G. Influence of Symmetry on the Luminescence and Radiative Lifetime of Nine-Coordinate Europium Complexes. *Inorg. Chem.* **2015**, *54*, 9166–9173. [[CrossRef](#)]

50. Moreau, P.; Colette-Maatouk, S.; Vitorge, P.; Gareil, P.; Reiller, P.E. Complexation of europium(III) by hydroxybenzoic acids: A time-resolved luminescence spectroscopy study. *Inorganica Chim. Acta* **2015**, *432*, 81–88. [[CrossRef](#)]
51. Barkleit, A.; Kretzschmar, J.; Tsushima, S.; Acker, M. Americium(III) and europium(III) complex formation with lactate at elevated temperatures studied by spectroscopy and quantum chemical calculations. *Dalt. Trans.* **2014**, *43*, 11221–11232. [[CrossRef](#)]



© 2020 by the authors. Licensee MDPI, Basel, Switzerland. This article is an open access article distributed under the terms and conditions of the Creative Commons Attribution (CC BY) license (<http://creativecommons.org/licenses/by/4.0/>).